

CLIMATOLOGY

Seasonal prediction of Indian wintertime aerosol pollution using the ocean memory effect

Meng Gao^{1,2*}, Peter Sherman³, Shaojie Song², Yueyue Yu⁴, Zhiwei Wu⁵, Michael B. McElroy^{2,3*}

As China makes every effort to control air pollution, India emerges as the world's most polluted country, receiving worldwide attention with frequent winter (boreal) haze extremes. In this study, we found that the interannual variability of wintertime aerosol pollution over northern India is regulated mainly by a combination of El Niño and the Antarctic Oscillation (AAO). Both El Niño sea surface temperature (SST) anomalies and AAO-induced Indian Ocean Meridional Dipole SST anomalies can persist from autumn to winter, offering prospects for a prewinter forecast of wintertime aerosol pollution over northern India. We constructed a multivariable regression model incorporating El Niño and AAO indices for autumn to predict wintertime AOD. The prediction exhibits a high degree of consistency with observation, with a correlation coefficient of 0.78 ($P < 0.01$). This statistical model could allow the Indian government to forecast aerosol pollution conditions in winter and accordingly improve plans for pollution control.

INTRODUCTION

With close to half of the world's population and rapidly increasing energy consumption, East and South Asia have become the world's hot spots for aerosol pollution (1), posing threats to human health (2), climate (3), and the hydrological cycle (4). As China reforms factories and reduces coal consumption in response to citizen pressure, India's cities are now labeled the world's most polluted (5). While the decadal trend of aerosol loadings over India has been linked to anthropogenic activities (6), the year-to-year variability is modulated by meteorological conditions and variability in large-scale circulation patterns.

Stagnant weather conditions (e.g., low wind speeds, descending air, and compressed boundary layer) favoring rapid aerosol formation and accumulation serve as the major contributors to extreme aerosol pollution events (7, 8). Previous studies have linked poor ventilation and extreme haze in China with weakening of circulation in the East Asia winter monsoon (9), Arctic sea ice loss (10), the positive phase of the Pacific Decadal Oscillation (11), the El Niño–Southern Oscillation (12, 13), and variability in Pacific sea surface temperature (SST) (14, 15). Similar to the seasonality of haze in China, haze pollution events in India occur mostly in winter. However, the climate factors modulating its interannual variability remain undefined, contributing to complications in air quality management.

Information from the preceding seasons could be important in planning of air pollution control in India. Understanding the climate factors modulating the interannual variability of wintertime haze pollution would help foresee future ventilation conditions and thus contribute to long-term planning for air pollution control. Weather conditions and large-scale climate patterns usually exhibit precursor information or have memory effects persisting across seasons (16). Considering these linkages, we argue that it may be possible to offer useful advance projections of wintertime haze pollution for India, potentially up to several years in advance given the intensive ongoing efforts devoted to the possibility of de-

veloping useful seasonal to even interannual prediction of climate variability.

This study aims to elucidate the dominant climate patterns driving the interannual variability of wintertime aerosol pollution over northern India, where a large portion of the Indian population is based and where extreme wintertime haze events are common. We first applied an empirical orthogonal function (EOF) analysis to decompose the historical spatial distributions of detrended satellite aerosol optical depth (AOD) observed over northern India. The first two leading EOF modes can explain 69% of the observed variance, implicating decadal variations associated with El Niño and the Antarctic Oscillation (AAO). The SST patterns resulting from El Niño and the AAO can persist from autumn to winter (ocean “memory” effect). Statistical analyses and sensitivity simulations were conducted using the state-of-the-art Community Earth System Model version 2 (CESM 2) to investigate the physical mechanism responsible for the associations with El Niño and the AAO. A multivariable regression model was constructed and shown to be effective [correlation coefficient (r) = 0.78, $P < 0.01$] in predicting wintertime AOD over northern India using the features of El Niño and the AAO observed in the preceding autumn.

RESULTS

Spatial distribution and decadal trend of satellite-observed AOD in India

Severe aerosol pollution is observed commonly over northern India, as indicated by the spatial distributions of 16-year (2003–2018) averaged wintertime AOD (Fig. 1A). Over the period of 2003–2018, AOD values in India have experienced an overall enhancement, with the largest rates of increase observed in northern India (about 0.03 per year) (Fig. 1B). The area-averaged rate of increase for India as a whole is about 0.012 per year. Similar increases have been reported on the basis of surface and satellite measurements (6, 17). The decadal intensification is connected intimately with the growth of population, energy consumption, and related emissions, particularly in northern India (6). Over the interval of 2003–2017, population increased by 21% (18), energy consumption grew by 103% (19), and emissions of SO₂ nearly doubled (20). Although changes in emissions of aerosol precursors strongly affect aerosol pollution in India, the interannual variability of weather conditions and circulation is additionally influential.

¹Department of Geography, Hong Kong Baptist University, Kowloon Tong, Hong Kong SAR, China. ²School of Engineering and Applied Sciences, Harvard University, Cambridge, MA 02138, USA. ³Department of Earth and Planetary Sciences, Harvard University, Cambridge, MA 02138, USA. ⁴Key Laboratory of Meteorological Disaster, Ministry of Education, Nanjing University of Information Science and Technology, Nanjing 210044, China. ⁵Institute of Atmospheric Sciences, Fudan University, Shanghai 200438, China.

*Corresponding author. Email: mmgao2@hkbu.edu.hk (M.G.); mmbm@seas.harvard.edu (M.B.M.)

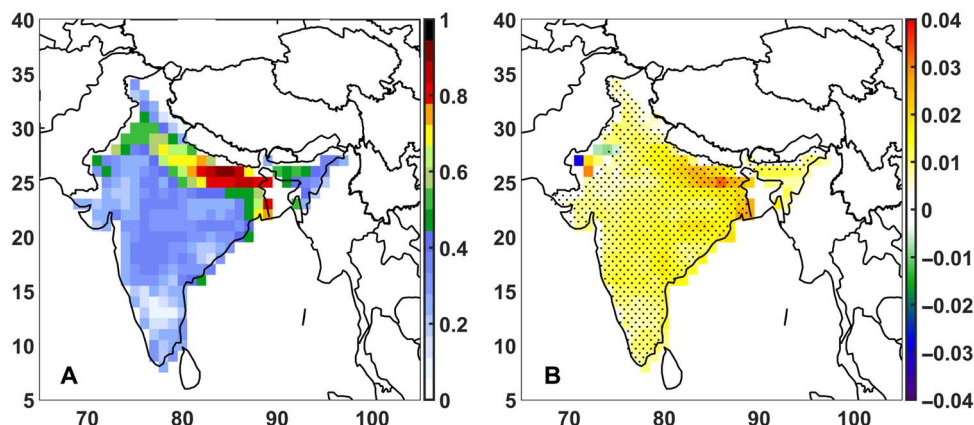


Fig. 1. Spatial features of mean wintertime AOD and trend. (A) The MODIS (Moderate Resolution Imaging Spectroradiometer) Terra/Aqua observed AOD at 550 nm in DJF (December, January, and February) averaged over 2003–2018 (December 2002, January 2003, and February 2003 are considered as winter of 2003). (B) DJF AOD trend (unitless/year) over 2003–2018 (black dots denote areas with significant trend; $P < 0.05$).

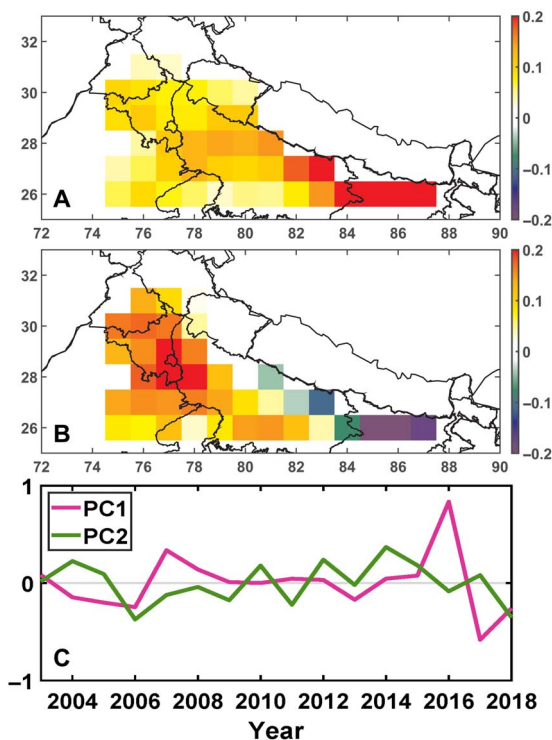


Fig. 2. Features of the first two leading modes. Spatial patterns of EOF1 (A), EOF2 (B), and PCs (C) of the two leading EOF modes.

Major modes of wintertime AOD over northern India

Since aerosol pollution is serious only in the north, our analysis is focused on northern India. To better investigate the driving climate patterns for Indian aerosol pollution, we detrended the satellite-measured AOD before applying EOF analysis. The EOF analysis indicates that the first and second leading modes (hereafter, EOF1 and EOF2) account for 46 and 23% of the total variance, respectively. According to the criterion proposed by North *et al.* (21), EOF1, EOF2, and EOF3 modes are statistically distinguishable (fig. S1), but we pay particular attention only to EOF1 and EOF2 in this study, as EOF3 makes a relatively smaller contribution to the total variance (fig. S1).

EOF3 is found to be negatively associated with the Arctic Oscillation (AO) (fig. S2), since positive AO can strengthen westerlies and precipitation during the Indian winter monsoon and thus alleviate pollution (22). As indicated in Fig. 2A, the spatial distribution of EOF1 exhibits a homogeneous positive feature, suggesting that the AOD values over northern India have the same pattern with respect to sensitivity. The corresponding principal component (PC1) shows strong interannual variability, with the highest value in 2016 and the lowest in 2017. EOF2 shows a zonal dipole pattern with positive sensitivity in the mid region and negative sensitivity to the east, indicating that the second component implies opposite patterns of impacts on aerosol pollution over the northcentral and northeast regions. The PC of EOF2 mode (PC2) reflects relatively weaker interannual variability as compared to PC1. These two major modes correspond to two different climate patterns influencing wintertime weather conditions and circulation in northern India.

To identify the climate patterns corresponding to the first two leading modes, we performed a correlation analysis with wintertime [December, January, and February (DJF)] SST. The resulting spatial pattern of correlation between PC1 and SST strongly resembles the pattern associated with El Niño, with warming located across the central and eastern Pacific, cooling over the western Pacific, and warming over the Indian Ocean (Fig. 3A). The correlation coefficients between PC1 and the Niño 1+2, Niño 3, and Niño 3.4 indices are 0.48 ($P < 0.05$), 0.55 ($P < 0.05$), and 0.51 ($P < 0.05$), respectively. However, PC1 does not correlate statistically with the Niño 4 index (0.31; $P > 0.05$), suggesting that PC1 contains less information with respect to the “Central Pacific-type El Niño.” El Niño-like SST anomalies exhibit usually good persistence from autumn to winter (23), as suggested by the significant correlation between PC1 and El Niño indices in the preceding autumn (0.52, 0.58, and 0.52 for Niño 1+2, Niño 3, and Niño 3.4 indices, respectively).

The resulting map of correlation between PC2 and wintertime SST indicates that regions exhibiting significant correlations (marked with black dots) are located mainly in the Southern Hemisphere (Fig. 3B), where climate is modulated dominantly by the AAO (24). PC2 does not correlate significantly with the AAO index in winter but with the AAO index in the preceding autumn (-0.59 ; $P < 0.05$), suggesting that the AAO pattern in the preceding season might exhibit a teleconnection with aerosol pollution over northern India.

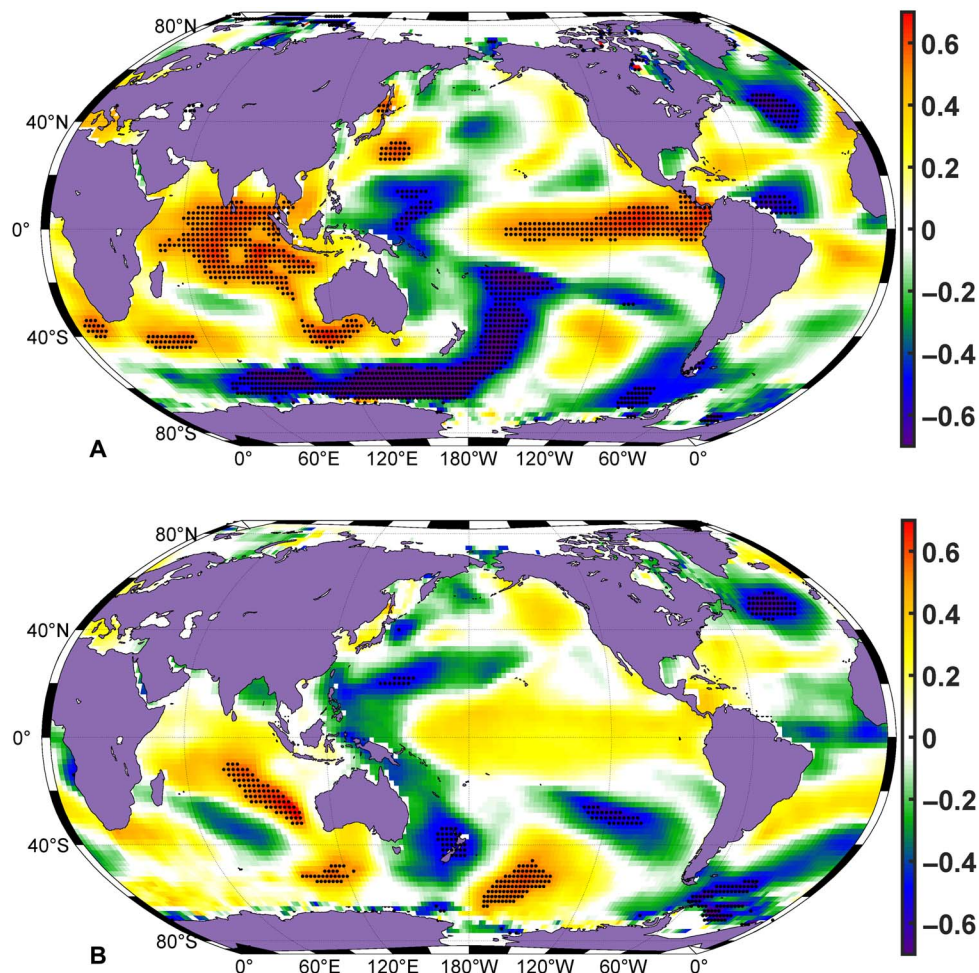


Fig. 3. Correlations between the first two modes and SST. (A) PC1-DJF SST correlation. (B) PC2-DJF SST correlation (black dots denote areas with significant correlation; $P < 0.05$).

Physical mechanisms

El Niño anomalies associated with Indian haze

As noted above, PC1 displays the strongest correlation with the Niño 3 index and statistically significant correlation with other Niño indices in both winter and the previous season. These results indicate that the SST pattern associated with El Niño can persist from autumn to winter (23). A warm tropical Pacific can result in diabatic heating, thus modulating the Walker circulation (25). These changes have been linked with the abnormal deepening of the East Asian trough and anomalous anticyclonic vorticity in South Asia (25). The influences on local wintertime weather conditions in northern India remain unexplored. Northern India is dominated by northwesterly winds (Fig. 4A) during winter, a consequence of the land-sea temperature contrast and the obstruction posed by the Tibetan Plateau. During strong El Niño winters, an abnormal cyclone is formed in the near-surface region, generating southeasterly winds opposite to the prevailing northwesterly winds over northern India. This weakening feature resulting from El Niño is also seen in the map of correlation between wind speeds at 10 m and the Niño 3 index. As shown in Fig. 4D, wind speeds are weaker in northern India during strong El Niño winters. Aerosol pollution is influenced both by horizontal winds and by boundary layer mixing, but we found that El Niño has little influence on the boundary heights over that region (fig. S3A). The

cyclone anomaly and the weakening of horizontal winds during strong El Niño winters appear to be responsible for the dependence on El Niño of the interannual variability of AOD over northern India.

To further verify the above assumption on how El Niño-like SST patterns influence local weather conditions and aerosol concentrations, we carried out a series of numerical experiments using the CESM 2 model, as described in the Materials and Methods section. The differences between CESM_{ElNiño} and CESM_{ctl} cases are considered to reflect the influence of El Niño, as shown in Fig. 5 (A and C). Consistent with the results from statistical analysis, an El Niño-like SST pattern can invigorate near-surface cyclone conditions in northern India, leading to weakening of near-surface wind speeds (Fig. 5A). The responses of aerosol concentrations are in line with the weakened winds, displaying enhanced values over nearly the entire India subcontinent (Fig. 5A). The simulated responses of AOD are generally consistent with the spatial distribution of EOF1, confirming the relationship between El Niño and aerosol pollution over northern India. The CESM Large Ensemble (LENS) datasets with 35 ensemble members also illustrate that the mean responses of AOD (fig. S7A) to El Niño are positive over India.

AAO anomalies associated with Indian haze

The interannual variability of wintertime AOD over northern India is also associated with the AAO in the preceding autumn but with

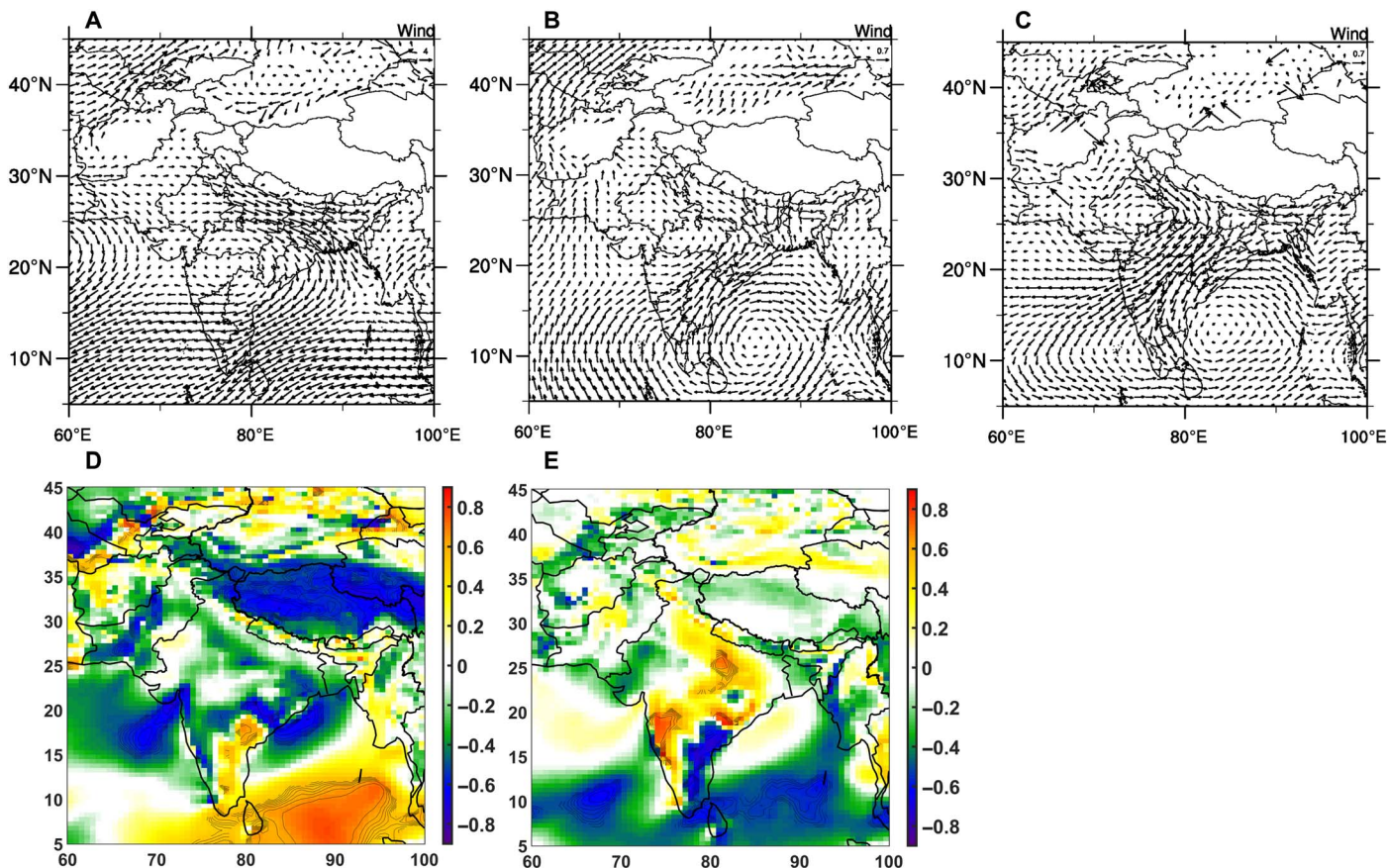


Fig. 4. Connections between wind fields and climate variability. (A) Winter winds averaged over 2003–2018 at 850 mbar. (B) Vector correlation map of winter winds at 850 mbar with reference to autumn Niño 3 index. (C) Vector correlation map of winter winds at 850 mbar with reference to Indian Ocean Meridional Dipole index (IOMDI). (D) Correlation map of winter wind speeds at 10 m with reference to autumn Niño 3 index. (E) Correlation map of winter wind speeds at 10 m with reference to IOMDI.

less dependence than the association with El Niño. Note that a strong (weak) AAO usually corresponds with the poleward (equatorward) movement of the high-level jet stream around the Antarctic (26, 27). Surface wind speeds vary in phase with movements of the high-level jet stream reflecting the equivalent barotropic structure of the AAO (28). The positive AAO is associated with a tripole feature in wind speeds at 10 m, in which winds decelerate near the Antarctic continent and near the equator but slow down in the southern midlatitudes (fig. S4). The anomalies in near-surface wind speeds can trigger anomalies in SST through latent heat exchange with high (low) wind speeds favoring lower (higher) SST (28). Consequently, positive SST anomalies develop at midlatitudes, with negative SST anomalies near the equator (fig. S5) (29–31). This dipole feature can persist from the preceding autumn to winter (fig. S5) and is proposed to influence the local circulation in India.

To quantitatively describe this dipole feature, we defined the Indian Ocean Meridional Dipole index (IOMDI) as the differences between the SST at midlatitudes and the SST near the equator. To further investigate the local anomalies in atmospheric circulation over India, we computed the vector correlations of winds at 850 mbar with reference to IOMDI (Fig. 4C). As noted above, northwesterly winds prevail over northern India in winter, and winters with high IOMDI excite stronger northwesterly winds over northcentral India but weaker westerly winds over northeastern India. This heterogeneous response is also confirmed in

the map of correlation between IOMDI and wind speeds at 10 m. Similarly, little influence was found between IOMDI and boundary layer heights (fig. S3B). Stronger near-surface winds over northcentral India and weakened winds over northeastern India associated with a positive AAO are favorable for dissipation of air pollutants over northcentral and accumulation over northwestern India.

To further explore the response of local circulation and concentrations of aerosols to the IOMD SST anomalies excited by the positive AAO, we conducted CESM 2 experiments imposing the IOMD SST feature. The differences between CESM_{AAO} and CESM_{ctl} cases are taken to reflect the influence of the positive AAO, as displayed in Fig. 5 (B and D). The dipole SST anomalies over the Indian Ocean can contribute to strengthening northerly winds over northcentral India with weaker westerly winds over northeastern India (Fig. 5B). The dipole SST anomalies can also lead to more precipitation in northcentral India with less precipitation in northeastern India (fig. S6). Accordingly, the response of aerosol concentrations is negative over northcentral India but positive over northeastern India (Fig. 5D). The simulated responses of AOD are generally consistent with the spatial distribution of EOF2, confirming the observed relationship between the AAO and aerosol pollution over northern India. The CESM LENS datasets with 35 ensemble members agree with our findings that positive autumn AAO is associated with heterogeneous responses of winter AOD over India (fig. S7B).

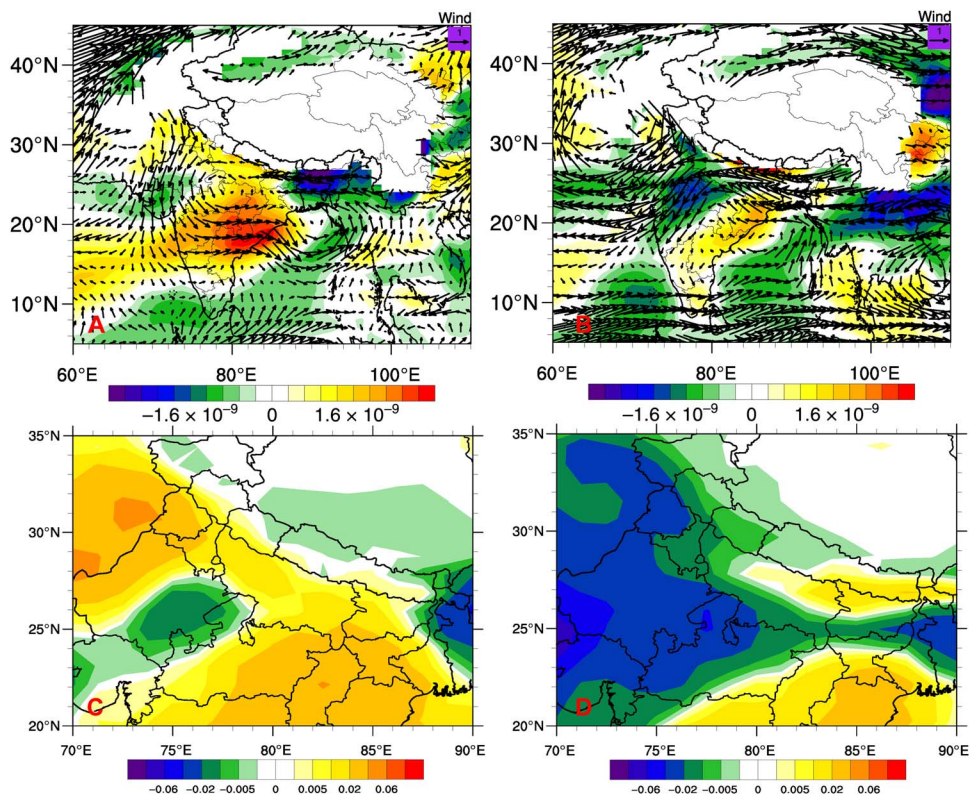


Fig. 5. CESM simulated responses of concentrations of near-surface aerosol and AOD. (A) CESM simulated response of concentrations of total particulate matter (kg/kg) and winds (reference, 1 m/s) at 850 mbar to El Niño-like SST. **(B)** CESM simulated response of concentrations of total particulate matter (kg/kg) and winds (reference, 1 m/s) at 850 mbar to IOMD-like SST. **(C)** CESM simulated response of AOD to El Niño-like SST. **(D)** CESM simulated response of AOD to IOMD-like SST.

Statistical model

Considering the significant correlation and the physical relationships linking climate indices for the preceding autumn with the leading modes of AOD over northern India, we were motivated to construct a statistical model to predict wintertime aerosol pollution over northern India using a combination of these indices. The multivariable linear regression models constructed using 15 combinations of four predictors (Niño 1+2, Niño 3, Niño 3.4, and AAO indices for September, October, and November) were compared using the Akaike information criterion (AIC), which is commonly used to assess the significance of statistical models with respect to effectiveness and the potential for overfitting. The model incorporating all four predictors performs best with the lowest AIC value of -75.31 (table S1). The different Niño indices are defined by changes observed in different regions of the tropical Pacific. It is true that the different indices are strongly correlated. It is reasonable, however, to expect that the Indian responses may be particularly sensitive to changes in particular regions of the tropical Pacific. Some pollution episodes may be connected with changes in the central Pacific, while others may be more sensitive to conditions in the eastern Pacific. To explore these possibilities, we considered all of the indices and found that the predictive capacity of the model is enhanced by considering a combination. As shown in Fig. 6, the statistical model could have been applied to have effectively predicted wintertime AOD (0.78 ; $P < 0.01$) as much as a season in advance, particularly during the strong El Niño winter of 2016 and the weak El Niño winters of 2017 and 2018.

To test the predictive capability of the built multivariable regression model, we performed a 10-fold cross-validation method (32) to

hindcast the AOD anomaly over northern India. The relevant procedures are as follows: Data during the period 2003–2018 were divided into 10 groups; each group was deleted to derive a forecast model using the remaining groups, and the deleted group was used to test the built forecast model. The correlation coefficient between observation and the 16-year cross-validated hindcast AOD anomaly is 0.54 ($P < 0.05$) (Fig. 6).

DISCUSSION

A number of studies have noted the link between climate patterns and wintertime aerosol pollution in China (9–15), yet the influence of climate patterns on aerosol pollution in the emerging most polluted country, India, has received much less attention. In this study, two major modes were identified using EOF analysis to describe the observed historical distribution of wintertime AOD over northern India. We attributed the first two leading modes to El Niño and the AAO, respectively, and examined the observed relationship between El Niño, the AAO, and aerosol pollution over northern India.

The influence of El Niño was linked to the distribution of absorbing aerosols over the Indian subcontinent through a mechanism in which warm SST anomalies during El Niño conditions enhance dust transport arising from convection over the Arabian Peninsula with subsidence over the subcontinent (33). Although the evidence provided is not sufficiently convincing absent a focused treatment of dust transport (33), the statistical relationship inferred between El Niño and aerosol pollution over India agrees with the findings in the current study.

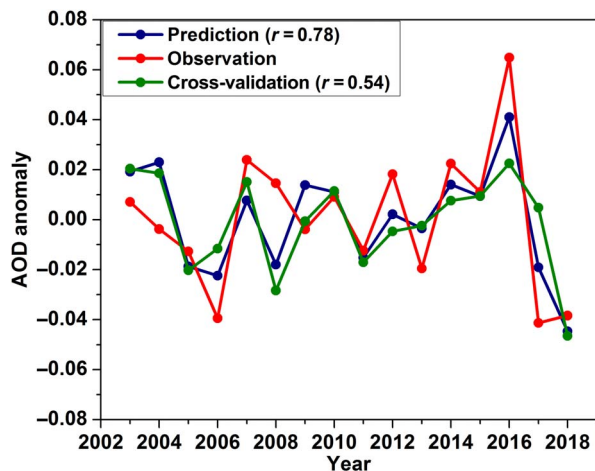


Fig. 6. Multivariable regression modeling. Time series of AOD anomaly for Northern India are represented in red. Results obtained using the regression model are indicated in blue. The hindcast AOD anomaly by the k -fold cross-validation method is denoted in green.

Under greenhouse warming, extreme El Niño events are projected to occur more frequently (34), suggesting prospects for deterioration of future weather and circulation conditions for air quality over northern India. Regional climate and chemistry model results also suggest that air pollution events in India are likely to increase, by 20 to 120 days per year in 2050 compared with present conditions (35).

The Indian government has not done much to tackle haze pollution issue. With increasing attention and pressure from the public, India could learn from China's experiences on this topic over the past 5 years. The findings in this study could help the Indian government foresee the ventilation conditions anticipated for winter in advance of the arrival of the winter season, and emission control plans could be implemented accordingly to minimize damage from potential deterioration in subsequent air quality.

Although the interannual variability was well described using the variation of El Niño and AAO, the severity of wintertime aerosol pollution over northern India is dominated still by the strength and temporal trends in emissions from anthropogenic activities. The influences of emissions on aerosol pollution are not discussed in this study but deserve careful attention for follow-up studies. Although efforts were made to quantify the emissions in India (36, 37), the species considered are limited, which poses problems for the development of instructive quantitative models. More comprehensive, homogenized, and publicly accessible emission inventories and observations are still urgently needed for India. These considerations highlight the need for a focused program of research to address these shortcomings.

MATERIALS AND METHODS

Satellite observations

We used the monthly gridded (1° by 1°) data on AOD at 550 nm, observed by the sensor MODIS (Moderate Resolution Imaging Spectroradiometer) aboard the Aqua and Terra satellites (combined Dark Target and Deep Blue algorithms, MYD08_M3 and MOD08_M3), to investigate the interannual variability of wintertime aerosol pollution over northern India covering the period 2003–2018 (year 2003 winter months include December of 2002, January of 2003, February of 2003,

and so on). MODIS provides near-global coverage every 1 to 2 days, with a 2330-km viewing swath. Terra passes from north to south across the equator in the morning, while Aqua passes south to north over the equator in the afternoon. The different local times at which Terra and Aqua pass over India introduce differences in retrieved AOD. We took the average of these two datasets to represent the mean pollution level. The retrievals adopted combine results from both Dark Target and Deep Blue algorithms, with the latter algorithm constructed specifically to retrieve AOD over desert regions.

Reanalysis, reconstructed SST, and climate indices

Monthly three-dimensional horizontal and vertical winds and boundary layer heights used in this study were obtained from the NASA Modern-Era Retrospective Analysis for Research and Applications, Version 2 (MERRA-2) dataset, a replacement for the MERRA dataset with more observational constraints. The MERRA-2 reanalysis is provided on a grid of 0.5° latitude by 0.625° longitude. The global SST records were taken from the National Oceanic and Atmospheric Administration (NOAA) Extended Reconstructed SST (ERSST) V5 dataset (38). ERSST, available on a 2° by 2° grid, was obtained from the International Comprehensive Ocean-Atmosphere Data Set (ICOADS). The latest version of ERSST, version 5, uses new datasets from ICOADS Release 3.0 SST, combining information from Argo floats above 5 m and Hadley Centre Ice-SST version 2 ice concentrations. The monthly El Niño and AAO indices over the period of 2003–2018 were taken from the NOAA website (www.esrl.noaa.gov/psd/data/climateindices/list/).

Statistical methods

EOF analysis was applied to decompose the satellite-observed wintertime AOD over northern India. EOF1 and EOF2 were well separated and distinct from higher modes according to the criteria suggested by North *et al.* (21). The decadal trend of AOD in India was computed using the linear regression slope. The significance of the trend was examined with Mann-Kendall trend analysis. The significance of the inferred correlation coefficients was tested using Student's t test.

A multivariable linear regression model was developed incorporating Niño 1+2, Niño 3, Niño 3.4, and AAO indices in autumn, using the following equation

$$\text{AOD} = a_1 I_{\text{Niño}1+2} + a_2 I_{\text{Niño}3} + a_3 I_{\text{Niño}3.4} + a_4 I_{\text{AAO}} + a_0$$

where a_0 , a_1 , a_2 , a_3 , and a_4 denote the coefficients determined through the multivariable regression procedure. The AIC was applied to evaluate the effectiveness of different combinations of model predictors. Detailed values of AIC for all 15 combinations were listed in table S1. The optimal model included Niño 1+2, Niño 3, Niño 3.4, and AAO indices since the corresponding AIC value was lowest in this case.

CESM experiments

We used the CESM 2 to establish the response of aerosol pollution over India to El Niño and AAO patterns, with 0.9° by 1.25° horizontal resolution and 32 vertical layers. The Community Atmosphere Model version 6 (CAM6) was used for the atmospheric component, and the Community Land Model version 5 was applied for the land component. CAM6 treats the processes and properties of major aerosol components, including sulfate, black carbon, primary organic matter, secondary organic aerosol, sea salt, and mineral dust, but simplified aerosol formation was applied, and oxidants were prescribed using historical simulations (39). Thus, the simulated aerosol modes might not

be as realistic as simulations using full chemistry description. We used simulated concentrations of aerosols to investigate the direction of the response to climate pattern perturbations in this study, instead of quantifying the magnitudes of the influences. Sea ice and SST were prescribed in the experiments using historically reconstructed SSTs. A control case was forced with SST data from monthly varying climatology (CESM_{ctl}). Two sensitivity cases were conducted by imposing an El Niño pattern (multiple-year composite) on SST (CESM_{ElNiño}) and by imposing the IOMD SST pattern (CESM_{AAO}) (multiple-year composite). All simulations were implemented starting in January 2010 and extending to May 2011. The results were analyzed for December of 2010 and for the first 2 months of 2011.

SUPPLEMENTARY MATERIALS

Supplementary material for this article is available at <http://advances.sciencemag.org/cgi/content/full/5/7/eaav4157/DC1>

Fig. S1. Fractional variance (%) explained by the first six EOF modes of winter AOD in Northern India.

Fig. S2. Interannual variability of DJF AO index and PC3.

Fig. S3. Correlation between boundary layer heights and Niño 3/IOMD indices.

Fig. S4. Correlation coefficients between the autumn AAO index and zonal mean wind speeds at 10 m in the Indian Ocean.

Fig. S5. Correlation between autumn AAO and autumn/winter SST.

Fig. S6. CESM simulated response of precipitation rate (m/s) to IOMD-like SST.

Fig. S7. Mean responses of AOD to El Niño and positive AAO using the outputs of CESM LENS simulations (35 ensemble members).

Table S1. AIC values for different combinations of predictors.

REFERENCES AND NOTES

- J. Lelieveld, P. J. Crutzen, V. Ramanathan, M. O. Andreae, C. A. M. Brenninkmeijer, T. Campos, G. R. Cass, R. R. Dickerson, H. Fischer, J. A. De Gouw, A. Hansel, A. Jefferson, D. Kley, A. T. J. de Laat, S. Lal, M. G. Lawrence, J. M. Lobert, O. L. Mayol-Bracero, A. P. Mitra, T. Novakov, S. J. Oltmans, K. A. Prather, T. Reiner, H. Rodhe, H. A. Scheeren, D. Sikka, J. Williams, The Indian Ocean experiment: Widespread air pollution from South and Southeast Asia. *Science* **291**, 1031–1036 (2001).
- J. Lelieveld, J. S. Evans, M. Fnais, D. Giannadaki, A. Pozzer, The contribution of outdoor air pollution sources to premature mortality on a global scale. *Nature* **525**, 367–371 (2015).
- V. Ramanathan, G. Carmichael, Global and regional climate changes due to black carbon. *Nat. Geosci.* **1**, 221–227 (2008).
- V. Ramanathan, P. J. Crutzen, J. T. Kiehl, D. Rosenfeld, Aerosols, climate, and the hydrological cycle. *Science* **294**, 2119–2124 (2001).
- World Health Organization Global Urban Ambient Air Pollution Database; www.who.int/phe/health_topics/outdoorair/databases/cities/en/ [accessed 13 September 2018].
- S. S. Babu, M. R. Manoj, K. K. Moorthy, M. M. Gogoi, V. S. Nair, S. K. Kompalli, S. K. Satheesh, K. Niranjana, P. K. Ramagopal, D. Bhuyan, D. Singh, Trends in aerosol optical depth over Indian region: Potential causes and impact indicators. *J. Geophys. Res. Atmos.* **118**, 11794–11806 (2013).
- M. Gao, G. R. Carmichael, Y. Wang, P. E. Saide, M. Yu, J. Xin, Z. Liu, Z. Wang, Modeling study of the 2010 regional haze event in the North China Plain. *Atmos. Chem. Phys.* **16**, 1673–1691 (2016).
- P. Wu, Y. Ding, Y. Liu, Atmospheric circulation and dynamic mechanism for persistent haze events in the Beijing–Tianjin–Hebei region. *Adv. Atmos. Sci.* **34**, 429–440 (2017).
- F. Niu, Z. Li, C. Li, K.-H. Lee, M. Wang, Increase of wintertime fog in China: Potential impacts of weakening of the Eastern Asian monsoon circulation and increasing aerosol loading. *J. Geophys. Res. Atmos.* **115**, D00K20 (2010).
- Y. Zou, Y. Wang, Y. Zhang, J.-H. Koo, Arctic sea ice, Eurasia snow, and extreme winter haze in China. *Sci. Adv.* **3**, e1602751 (2017).
- S. Zhao, J. Li, C. Sun, Decadal variability in the occurrence of wintertime haze in central eastern China tied to the Pacific Decadal Oscillation. *Sci. Rep.* **6**, 27424 (2016).
- G. Hui, L. Xiang, Influences of El Niño Southern Oscillation events on haze frequency in eastern China during boreal winters. *Int. J. Climatol.* **35**, 2682–2688 (2015).
- J. Feng, J. Li, J. Zhu, H. Liao, Influences of El Niño Modoki event 1994/1995 on aerosol concentrations over southern China. *J. Geophys. Res. Atmos.* **121**, 1637–1651 (2016).
- L. Pei, Z. Yan, Z. Sun, S. Miao, Y. Yao, Increasing persistent haze in Beijing: Potential impacts of weakening East Asian winter monsoons associated with northwestern Pacific sea surface temperature trends. *Atmos. Chem. Phys.* **18**, 3173–3183 (2018).
- Z. Yin, H. Wang, The relationship between the subtropical Western Pacific SST and haze over North-Central North China Plain. *Int. J. Climatol.* **36**, 3479–3491 (2016).
- R. Vautard, Multiple weather regimes over the North Atlantic: Analysis of precursors and successors. *Mon. Weather Rev.* **118**, 2056–2081 (1990).
- S. S. Pijthi, P. V. N. Rao, M. Mohan, M. V. R. S. Sai, M. V. Ramana, Trends of absorption, scattering and total aerosol optical depths over India and surrounding oceanic regions from satellite observations: Role of local production, transport and atmospheric dynamics. *Environ. Sci. Pollut. Res.* **25**, 18147–18160 (2018).
- The World Bank Population Data; <https://data.worldbank.org/indicator/sp.pop.totl> [accessed 13 September 2018].
- Global Energy Statistical Yearbook 2018; <https://yearbook.enerdata.net/total-energy/world-consumption-statistics.html> [accessed 13 September 2018].
- C. Li, C. McLinden, V. Fioletov, N. Krotkov, S. Carn, J. Joiner, D. Streets, H. He, X. Ren, Z. Li, R. R. Dickerson, India is overtaking China as the world's largest emitter of anthropogenic sulfur dioxide. *Sci. Rep.* **7**, 14304 (2017).
- G. R. North, T. L. Bell, R. F. Cahalan, F. J. Moeng, Sampling errors in the estimation of empirical orthogonal functions. *Mon. Weather Rev.* **110**, 699–706 (1982).
- T. M. Midhuna, A. P. Dimri, Impact of arctic oscillation on Indian winter monsoon. *Meteorol. Atmos. Phys.* **2018**, 1–11 (2018).
- C. Torrence, P. J. Webster, The annual cycle of persistence in the El Niño/Southern Oscillation. *Q. J. R. Meteorol. Soc.* **124**, 1985–2004 (1998).
- D. Gong, S. Wang, Definition of Antarctic oscillation index. *Geophys. Res. Lett.* **26**, 459–462 (1999).
- B. Wang, Q. Zhang, Pacific–east Asian teleconnection. Part II: How the Philippine Sea anomalous anticyclone is established during El Niño development. *J. Clim.* **15**, 3252–3265 (2002).
- D. W. J. Thompson, J. M. Wallace, Annular modes in the extratropical circulation. Part I: Month-to-month variability. *J. Clim.* **13**, 1000–1016 (2000).
- D. W. J. Thompson, J. M. Wallace, G. C. Hegerl, Annular modes in the extratropical circulation. Part II: Trends. *J. Clim.* **13**, 1018–1036 (2000).
- Z. Wu, J. Li, B. Wang, X. Liu, Can the Southern Hemisphere annular mode affect China winter monsoon? *J. Geophys. Res. Atmos.* **114**, D11107 (2009).
- J. Li, Impacts of annular modes on extreme climate events over the East Asian monsoon region, in *Dynamics and Predictability of Large-Scale, High-Impact Weather and Climate Events* (Cambridge Univ. Press, 2016), pp. 341–353.
- T. Liu, J. Li, F. Zheng, Influence of the boreal autumn Southern Annular Mode on winter precipitation over land in the Northern Hemisphere. *J. Clim.* **28**, 8825–8839 (2015).
- T. Liu, J. Li, J. Feng, X. Wang, Y. Li, Cross-seasonal relationship between the boreal autumn SAM and winter precipitation in the Northern Hemisphere in CMIP5. *J. Clim.* **29**, 6617–6636 (2016).
- Z. Wu, B. Wang, J. Li, F.-F. Jin, An empirical seasonal prediction model of the East Asian summer monsoon using ENSO and NAO. *J. Geophys. Res. Atmos.* **114**, D18120 (2009).
- B. Abish, K. Mohanakumar, Absorbing aerosol variability over the Indian subcontinent and its increasing dependence on ENSO. *Glob. Planet. Change* **106**, 13–19 (2013).
- W. Cai, A. Santoso, G. Wang, S.-W. Yeh, S.-I. An, K. M. Cobb, M. Collins, E. Guilyardi, F.-F. Jin, J.-S. Kug, M. Lengaigne, M. J. McPhaden, K. Takahashi, A. Timmermann, G. Vecchi, M. Watanabe, L. Wu, ENSO and greenhouse warming. *Nat. Clim. Change* **5**, 849–859 (2015).
- R. Kumar, M. C. Barth, G. G. Pfister, L. Delle Monache, J. F. Lamarque, S. Archer-Nicholls, S. Tilmes, S. D. Ghude, C. Wiedinmyer, M. Naja, S. Walters, How will air quality change in South Asia by 2050? *J. Geophys. Res. Atmos.* **123**, 1840–1864 (2018).
- M. S. Reddy, C. Venkataraman, Inventory of aerosol and sulphur dioxide emissions from India: I—Fossil fuel combustion. *Atmos. Environ.* **36**, 677–697 (2002).
- C. Venkataraman, G. Habib, A. Eiguren-Fernandez, A. H. Miguel, S. K. Friedlander, Residential biofuels in South Asia: Carbonaceous aerosol emissions and climate impacts. *Science* **307**, 1454–1456 (2005).
- B. Huang, P. W. Thorne, V. F. Banzon, T. Boyer, G. Chepurin, J. H. Lawrimore, M. J. Menne, T. M. Smith, R. S. Vose, H.-M. Zhang, Extended reconstructed sea surface temperature, version 5 (ERSSTv5): Upgrades, validations, and intercomparisons. *J. Clim.* **30**, 8179–8205 (2017).
- J. F. Lamarque, L. K. Emmons, P. G. Hess, D. E. Kinnison, S. Tilmes, F. Vitt, C. L. Heald, E. A. Holland, P. H. Lauritzen, J. Neu, J. J. Orlando, CAM-chem: Description and evaluation of interactive atmospheric chemistry in the Community Earth System Model. *Geosci. Model Dev.* **5**, 369–411 (2012).

Acknowledgments: We acknowledge NASA for providing the MODIS measurements and the MERRA-2 reanalysis dataset. We thank the National Center for Atmospheric Research for providing computational resources. **Funding:** This study was supported by the Harvard Global

Institute. **Author contributions:** M.G. and M.B.M. conceived the research. M.G. and P.S. analyzed measurements and conducted model simulations. S.S., Y.Y., and Z.W. assisted with the discussion. All authors contributed to the final interpretation and writing of the manuscript with major contributions by M.G., P.S., and M.B.M. **Competing interests:** The authors declare that they have no competing interests. **Data and materials availability:** All data needed to evaluate the conclusions in the paper are present in the paper and/or the Supplementary Materials. Additional data related to this paper may be requested from the authors.

Submitted 13 September 2018

Accepted 11 June 2019

Published 17 July 2019

10.1126/sciadv.aav4157

Citation: M. Gao, P. Sherman, S. Song, Y. Yu, Z. Wu, M. B. McElroy, Seasonal prediction of Indian wintertime aerosol pollution using the ocean memory effect. *Sci. Adv.* **5**, eaav4157 (2019).

Seasonal prediction of Indian wintertime aerosol pollution using the ocean memory effect

Meng Gao, Peter Sherman, Shaojie Song, Yueyue Yu, Zhiwei Wu and Michael B. McElroy

Sci Adv 5 (7), eaav4157.

DOI: 10.1126/sciadv.aav4157

ARTICLE TOOLS

<http://advances.sciencemag.org/content/5/7/eaav4157>

SUPPLEMENTARY MATERIALS

<http://advances.sciencemag.org/content/suppl/2019/07/15/5.7.eaav4157.DC1>

REFERENCES

This article cites 35 articles, 4 of which you can access for free
<http://advances.sciencemag.org/content/5/7/eaav4157#BIBL>

PERMISSIONS

<http://www.sciencemag.org/help/reprints-and-permissions>

Use of this article is subject to the [Terms of Service](#)

Science Advances (ISSN 2375-2548) is published by the American Association for the Advancement of Science, 1200 New York Avenue NW, Washington, DC 20005. The title *Science Advances* is a registered trademark of AAAS.

Copyright © 2019 The Authors, some rights reserved; exclusive licensee American Association for the Advancement of Science. No claim to original U.S. Government Works. Distributed under a Creative Commons Attribution NonCommercial License 4.0 (CC BY-NC).